Polymer 254 (2022) 125078

Contents lists available at ScienceDirect

Polymer

journal homepage: www.elsevier.com/locate/polymer

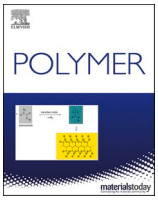

Heat-resistant colorless polyimides from benzimidazole diamines: Synthesis and properties

Dandan Li [a], Chengyang Wang [a], Xiaoying Yan [b], Shengqi Ma [a], Ran Lu [a], Guangtao Qian [b,*], Hongwei Zhou [a,**]

[a] College of Chemistry, Jilin University, Changchun, 130012, PR China
[b] Center for Advanced Low-Dimension Materials, State Key Laboratory for Modification of Chemical Fibers and Polymer Materials, College of Material Science and Engineering, Donghua University, Shanghai, 201620, PR China

ARTICLE INFO

Keywords:
Colorless poyimide
Poly(benzimidazole imide)s
Superheat-resistance

ABSTRACT

To prepare colorless polyimides (CPIs), two novel diamines, namely 6-amino-2-(2′-methyl-4′-aminobenzene)-N-phenylbenzimidazol (5a) and 6-amino-2-(2′-trifluoromethyl-4′-aminobenzene)-N-phenylbenzimidazol (5b) were synthesized, and two series of polyimides derived from them were developed. Except for the inherent asymmetric structures, the twisted moieties had been successfully incorporated in the benzimidazole dianmines through 2′- and N-substituents. The loose chain packing and hindered charge transfer (CT) interaction caused by the askew and distorted segments provided the polyimides with excellent optical transparency (80% transmittance at 400 nm, semi-alicyclic series), while the resulting films inherited the unique superheat-resistance of poly(benzimidazole imide)s (PBIIs), e.g., high glass-transition temperatures (up to 402 °C). Such outstanding optical and thermal properties expanded their application as heat-resistant colorless materials. Furthermore, the correlation between various 2′-substituents and characters of these PBII films was systematically analyzed. These data indicated that these colorless polyimides had potential application as optical and optoelectronic materials.

1. Introduction

Optically transparent films with inherent flexibility and light weight have attracted intensive attention because of the rapidly increasing demand in the fields of flexible display substrates and optoelectronic window films [1,2]. Despite excellent optical transparency, such polymers need to take into account high thermal properties to withstand the severe temperature (400 °C, short term) during manufacturing processes [3,4]. Most plastics with good optical transparency, such as poly(ether sulfone) (T_g = ~225 °C), polycarbonate (T_g = ~145 °C) or polyethylene naphthalate (T_g = ~120 °C) are restricted to be used in advanced optoelectronic engineering because of their limited service temperatures [5]. Thus, optically transparent polymers with superior heat resistance are required urgently in engineering and science [6,7]. Polyimides rank among most heat-resistant polymers widely used as high temperature polymers with extremely high glass transition temperature (T_g) and thermal decomposition temperature (T_d) [8–10]. However, the available polyimides usually illustrate poor optical transmittance and deep colors originating from the intra- and inter-molecular charge transfer complexes (CTC) formation, which is the main hindrance for their applications in optical and optoelectronic fields [11–13].

Current research has proven that the CTC can be hampered by the loose chain packing, disturbed conjugations along with the suppression of electron-donating (diamine) and electron-withdrawing (dianhydride) ability, achieving colorless polyimides [14–17]. According to the efficient approaches, various rational structural manipulations have been implemented, including the introduction of noncoplanar segments, asymmetric moieties, bulky substituents, alicyclic units, trifluoromethyl (-CF_3) groups and flexible structures [18–21]. Among many diamines monomers used in polyimide synthesis, benzimidazole diamine, namely 5(6)-amino-2-(4-aminobenzene)benzimidazole (PABZ), possesses a unique asymmetric structure [22,23]. With the inherently asymmetric and rigid diamines, poly(benzimidazole imide)s are expected to improve not only thermal properties but also optical transparency. Nonetheless, in past few decades, poly(benzimidazole imide)s have been researched as thermal-resistant fabrications but cannot be employed as optical

* Corresponding author.
** Corresponding author.
E-mail addresses: qgt@dhu.edu.cn (G. Qian), zhw@jlu.edu.cn (H. Zhou).

https://doi.org/10.1016/j.polymer.2022.125078
Received 15 April 2022; Received in revised form 13 June 2022; Accepted 14 June 2022
Available online 27 June 2022

materials [24–27]. The primary reason is that the incorporation of hydrogen bonds, which comes from a proton donor (N–H group) of benzimidazole moieties, enhances intermolecular packing coefficients and CT interaction [28,29]. Thus, PBII films often exhibit a dark brown color, limiting their application in optical device. In our previous study, incorporating a bulky N-phenyl unit can effectively reduce chain packing coefficient and obstruct H-bonding formation, providing the optimized poly(benzimidazole imide)s with enhanced optical transparency and high heat resistance [30].

In this study, two 2′-substituted N-phenyl-benzimidazole diamines, 6-amino-2-(2′-methyl-4′-aminobenzene)-N-phenylbenzimidazol (5a) and 6-amino-2-(2′-trifluoromethyl-4′-aminobenzene)-N-phenylbenzimidazol (5b), were synthesized (Scheme 1). The non-planar structures resulted from N-phenyl and 2′-substituents may provide more chances for colorless PBIIs formation. Semi- and fully aromatic PBII films were prepared through a one-stage method (Scheme 2), and the correlation between various 2′-substituents and properties of these poly(benzimidazole imide)s was systematically discussed. This work attempted to obtain colorless PBIIs to achieve heat-resistant colorless materials.

2. Experimental

2.1. Materials

2,4-dinitro-N-phenylaniline, 2-methyl-4-nitrobenzoic acid, 2-trifluoromethy-4-nitrobenzoic acid and isoquinoline were procured and used as received from Shanghai Haohong Biomedical Technology Co.: Ltd. 2,2′-bis(3,4-dicarboxyphenyl)hexafluoropropane dianhydride (6FDA), 1,2,4,5-cyclohexanetetracarboxylic dianhydride (HPMDA) were from TCI Co.: Ltd. Triethylamine, Sodium sulfide (Na_2S), Sodium bicarbonate ($NaHCO_3$), 80% hydrazine monohydrate, 10% palladium on charcoal, *p*-Toluenesulfonic acid (*p*-TSA) and other reagents were provided by Sinopharm Chemical Reagent Beijing Co. Ltd. 1,4-Butyrolactone (GBL), *N*,*N*-dimethylacetamide (DMAc) and *m*-cresol were purified by vacuum distillation prior to use. All monomers were dried at 80 °C in a vacuum oven for 24 h to eliminate the effect of water before use.

2.2. Measurements

^{1}H NMR and ^{1}H–^{1}H COSY spectra were obtained on a Bruker 600 AVANCE III spectrometer in dimethyl sulfoxide-d_6. Elemental analyses were executed on Elmentar Vario EL-III. The chemical structures of monomers were monitored on a Nicolet 6700 infrared spectrometer and the characterization of films was detected in attenuated total reflectance (ATR) mode. Inherent viscosity (η_{inh}) was measured with an Ubbelohde viscometer at 25 ± 0.1 °C at a concentration of 0.5 g/dL in DMAc. The number average (M_n) and weight-average (M_w) molecular weights were estimated by using Waters GPC Systems with a polystyrene standard calibration curve. Colour intensity was evaluated by a Hangzhou color spectrum CS-720 colorimeter with an observational angle of 10°. Ultraviolet (UV) visible spectra were recorded using a Shimadzu UV-3600

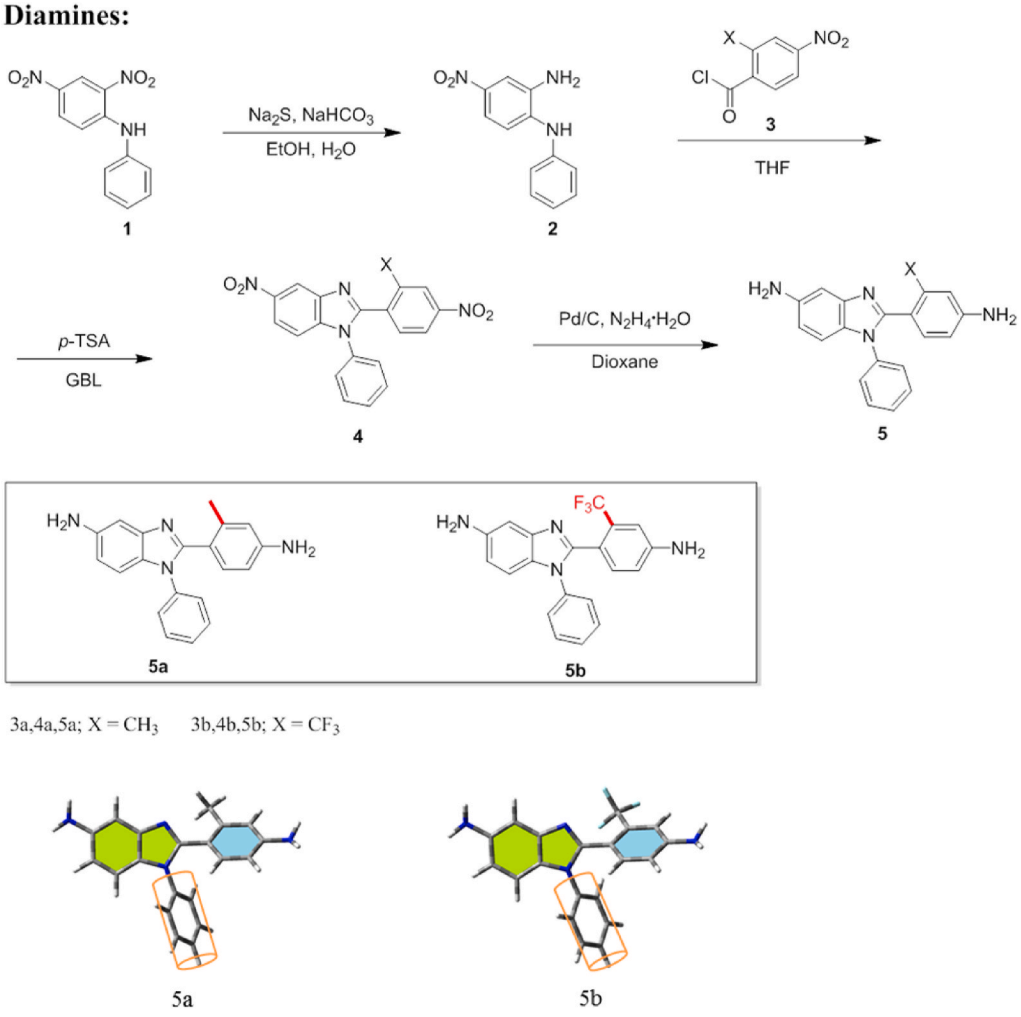

Scheme 1. Synthetic route to the benzimidazole diamines (geometrical structures were calculated by Gaussian 09W).

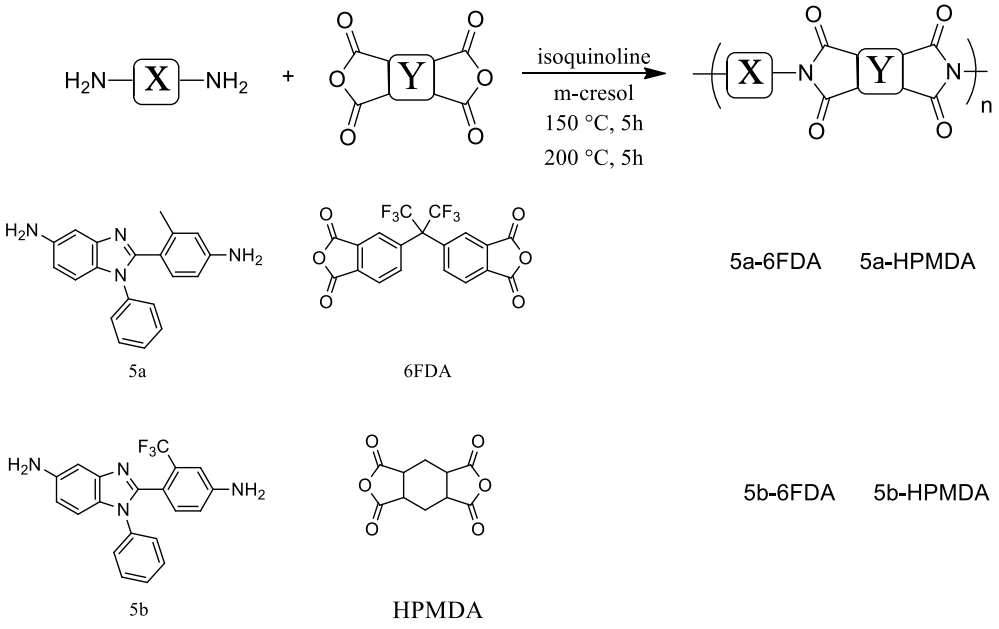

Scheme 2. Synthetic routes to the poly(benzimidazole imide)s.

spectrophotometer in the wavelength range of 200–700 nm. Wide-angle X-ray diffraction (WAXD) were collected on a Rigaku Denki D/MAX-2500 diffractometer with Cu Kα radiation (λ = 1.54 Å) at room temperature. The thermogravimetric analysis was assessed using Discovery TGA 550 with a constant heating rate of 10 °C min^{-1} under nitrogen. Mechanical properties of polymer films were evaluated on an Instron 5966 universal testing machine at speed of 5 mm min^{-1}, and tensile modulus (E), tensile strength (σ), and elongation at break (ε) were demonstrated as the average of five strips. Dynamic mechanical analysis (DMA) was performed on a TA Instrument DMA Q800 with a heating rate of 5 °C min^{-1} and a frequency of 1 Hz. Coefficient of thermal expansion (CTE) was collected using a TA Instrument TMA Q400 at a heating rate of 5 °C min^{-1}. Solubility was determined by dissolving 10 mg of the polyimide sample in 1 mL of the corresponding solvents at 25 °C for 24 h. The energy-optimized structures of the diamines and net charges of their terminal amino groups were achieved through the B3LYP (Becke, three-parameter, Lee–Yang–Parr) exchange-correlation functional for the 6-311G (d, p) basis set basis set in Gaussian 09W.

2.3. Synthesis of diamines

2.3.1. 6-nitro-2-(2′-methyl-4′-nitrobenzene)-N-phenylbenzimidazol (4a)

2-methyl-4-nitrobenzoyl chloride (10.4 g, 0.052 mol, synthetic routes was given in the supporting information) in THF (50.0 mL) was added to a solution of N-(2-amino-4-nitrophenyl)-N-phenylamine (10.0 g, 0.044 mol, synthetic routes was given in the supporting information) and triethylamine (5.3 g, 0.052 mol) in THF (50.0 mL) at 0 °C. The reaction was warmed to room temperature, stirred for 6 h, and quenched with 200 mL water. After filtration by suction, the resulting powder was dried at 80 °C in vacuum. Under a nitrogen atmosphere, the product was dissolved in GBL (200.0 mL), then, *p*-TSA (9.0 g, 0.052 mol) was added and the mixture was heated under reflux for 6 h. The reaction mixture was cooled and water (400.0 ml) was added. The precipitated powder was collected by filtration and recrystallized with mixed solvent (dioxane: H_2O = 5 : 1). A light brown powder was obtained (14.2 g, yield: 86.0%). Melting point: 207.5 °C. ^{1}H NMR (DMSO-d_6, ppm): δ = 8.75 (d, 1H, J = 1.8 Hz), 8.27 (dd, 1H, J = 9.0, 1.9 Hz), 8.21 (d, 1H, J = 5.1 Hz), 8.04 (dd, 1H, J = 8.5, 1.8 Hz), 7.67 (d, 1H, J = 8.5 Hz), 7.55–7.47 (m, 6H), 2.36 (s, 3H). FTIR (KBr, ν, cm^{-1}): 1617, 1594 (C═N/C═C stretching of ring), 1520, 1352 (NO_2 asymmetric and symmetric stretching). Anal. Calcd for $C_{20}H_{14}N_4O_4$: C, 64.17; H, 3.77; N, 14.97. Found: C, 64.01; H, 3.56; N, 15.02.

2.3.2. 6-nitro-2-(2′-trifluoromethyl-4′-nitrobenzene)-N-phenylbenzimidazol (4b)

The synthetic manner was similar to that used for 4a except that 2-trifluoromethyl-4-nitrobenzoyl chloride (3b, synthetic routes was given in the supporting information) played as a raw material. A light brown powder (yield: 84.2%). Melting point: 230.9 °C. ^{1}H NMR (DMSO-d_6, ppm): δ = 8.79 (d, 1H, J = 4.7 Hz), 8.59 (d, 1H, J = 5.0 Hz), 8.55 (dd, 1H, J = 8.6, 4.6 Hz), 8.29 (dd, 1H, J = 9.1, 4.6 Hz), 8.09 (dd, 1H, J = 8.5, 3.3 Hz), 7.58–7.48 (m, 4H), 7.45 (t, 2H, J = 6.0 Hz). FTIR (KBr, ν, cm^{-1}): 1617, 1594 (C═N/C═C stretching of ring), 1520, 1352 (NO_2 asymmetric and symmetric stretching). Anal. Calcd for $C_{20}H_{11}F_3N_4O_4$: C, 56.08; H, 2.59; N, 13.08. Found: C, 56.21; H, 2.48; N, 13.18.

2.3.3. 6-amino-2-(2′-methyl-4′-aminobenzene)-N-phenylbenzimidazol (5a)

To a refluxing mixture of 4a (10, 0.027 mol) and Pd/C (10%, 1.0 g) in 100 mL dioxane was added hydrazine hydrate (80%, 20 mL) over a 1-h period. The reaction was refluxed 6 h, cooled, and filtered through diatomaceous earth. The mother liquor was poured into water and filtered. The precipitation was wash with ethanol and recrystallized from a DMSO-water (1:1) mixture to give a white powder (7.9 g, yield: 93.1%). Melting point: 216.0 °C. ^{1}H NMR (DMSO-d_6, ppm): δ = 7.43 (t, 2H, J = 7.8 Hz), 7.35 (d, 1H, J = 7.4 Hz), 7.25–7.18 (m, 2H), 6.96 (d, 1H, J = 8.5 Hz), 6.85 (d, 1H, J = 2.0 Hz), 6.83 (d, 1H, J = 8.2 Hz), 6.58 (dd, 1H, J = 8.5, 2.1 Hz), 6.36 (d, 1H, J = 2.0 Hz), 6.28 (dd, 1H, J = 8.2, 2.2 Hz), 5.25 (s, 2H), 4.84 (s, 2H), 2.01 (s, 3H). FTIR (KBr, ν, cm^{-1}): 3457, 3339, 3176 (amine NH), 1628, 1608 (C═N/C═C stretching of ring). Anal. Calcd for $C_{20}H_{18}N_4$: C, 76.41; H, 5.77; N, 17.82. Found: C, 76.39; H, 5.85; N, 17.52.

2.3.4. 6-amino-2-(2′-trifluoromethyl-4′-aminobenzene)-N-phenylbenzimidazol (5b)

5b was prepared by reduction of 4a using the above procedure. A white powder (yield: 91.2%). Melting point: 100.1 °C. ^{1}H NMR (DMSO-d_6, ppm): δ = 7.44 (t, 2H, J = 7.8 Hz), 7.35 (d, 1H, J = 7.5 Hz), 7.20 (d, 2H, J = 7.4 Hz), 7.07 (d, 1H, J = 8.4 Hz), 6.92 (d, 1H, J = 8.6

Hz), 6.89 (d, 1H, $J = 2.3$ Hz), 6.85 (d, 1H, $J = 1.9$ Hz), 6.65 (dd, 1H, $J =$ 8.4, 2.2 Hz), 6.61 (dd, 1H, $J = 8.6$, 2.1 Hz), 5.85 (s, 2H), 4.87 (s, 2H). FTIR (KBr, ν, cm^{-1}): 3468, 3328, 3220 (amine NH), 1642, 1615 (C═N/C═C stretching of ring). Anal. Calcd for $C_{20}H_{15}F_3N_4$: C, 65.21; H, 4.10; N, 15.21. Found: C, 65.11; H, 4.21; N, 15.32.

2.4. Synthesis of polymers

The resulting PBIIs were synthesized through a one-stage method in *m*-cresol with isoquinoline. The representative processes were showed as follows.

HPMDA (0.3565 g, 1.590 mmol) and 5a (0.5 g, 1.590 mmol) was charged in a solution of *m*-cresol (4.9 g) under nitrogen atmosphere in the 20 mL three-necked flask equipped with a mechanical stirrer. The reaction solution was stirred at 150 °C for 5 h, then, isoquinoline (0.0411 g, 0.318 mmol) was added and the mixture was kept stirring at 180 °C for additional 5 h. After the polycondensation completed, the reaction was cooled to room temperature and poured into 100 ml ethanol. The fibrous polyimide appeared. Before being was dried under vacuum, the polymer was repeatedly dipped in ethanol to remove excess *m*-cresol. A white fibrous 5a-HPMDA (0.7449 g, yield 93.2%) was collected by filtration. The polyimide was re-dissolved in DMAc (5 wt%), followed by, the solution cast on a dust-free glass disc after being filtered through a 1.0 μm PTFE filter. The glass plate was placed in an oven at 160 °C overnight to deplete the solvent. Finally, the polyimide film was peeled off from the disc after immersion in boiling water.

3. Results and discussion

3.1. Monomer structure

Two N-phenyl benzimidazole containing different 2′-substituents were successfully synthesized (Scheme 1), and their structures were distinguished by FTIR spectroscopy (Fig. S1), ^{1}H NMR (Fig. 1 and Fig. S2), ^{1}H–^{1}H COSY (Fig. S3) elemental analysis. In the results, all of diamines had characteristic absorptions of the –NH_2 stretching bands (3385-3202 cm^{-1}) in the FTIR spectrum and two obvious signals of amine proton located at near 5.55 and 4.85 in ^{1}H NMR, which explained the typical diamine structures were got really. As shown in Fig. 1, the shift occurred for the amine protons linked to benzimidazole ring (H-12) highlighted the strong resonance caused by the electron-donating effect of 2′-methyl (5a) and the electron-withdrawing effect of 2′-trifluoromethyl (5b). It also inferred that 5a would possess higher nucleophilicity than 5b. In addition, these diamines features in their ^{1}H–^{1}H COSY spectra (Fig. S3) were fully assigned, confirming the expected structure.

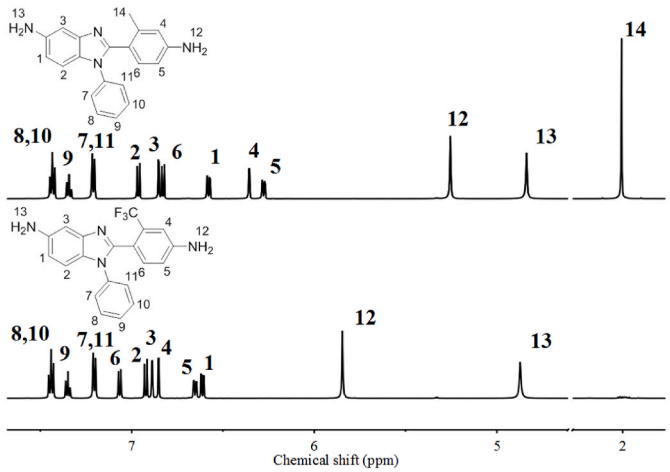

Fig. 1. ^{1}H NMR spectra of the benzimidazole diamines (5a and 5b).

In order to further understand the characteristics of these diamine structures, their geometries and net charges were calculated by the DFT [B3LYP/6-311G(d,p)] embedded in the Gaussian 09W software (Fig. 2). As expected, the N atom of amines attached to the 2′-methyl phenyl ring showed higher net charges than the one attached to the 2′-trifluoromethyl phenyl ring, which conformed to the features of ^{1}H NMR. Moreover, the dihedral angle between benzimidazole and N-phenyl (α) exhibited the same value of 60°. It suggested that the 2′-substituted methyl and trifluoromethyl did not significantly influence the geometries of N-substitution group. However, it could be seen that the model compounds gave the different dihedral angle (β) between imidazole ring and 2′-substituted phenyl. The β in the 5b was larger, which was indicative of much more noncoplanar segments, compared to 5a. That was, 5b with 2′-trifluoromethyl obviously twisted the polyimide chains. It implied that 5b-based PBIIs would possess higher optical transparency compared to the corresponding 5a-ones.

3.2. Polymerization characterization

To get sufficient molecular weights, the benzimidazole-containing PIs were synthesized through a one-step procedure in the presence of *m*-cresol and isoquinoline (Scheme 2). Their η_{inh} and M_n were in the range of 0.52–0.82 dL g^{-1} and 23.8–48.6 × 10^3 g mol^{-1} (Table S1), reflecting all of them possessed moderate molecular weights. Besides, the values of their number-average molecular weights followed the order: 5a-PBIIs > 5b-PBIIs, which were related the higher nucleophilicity of 5a compared to 5b. Normally, the higher electron-donating effect of terminal amino groups in the monomeric diamines would induce a higher degree of polycondensation, resulting in higher molecular weights. The trend was in agreement with the above-mentioned result of molecular modeling and ^{1}H NMR.

The poly(benzimidazole imide)s with anticipated chemical structures were successfully obtained, which was evidenced by ATR-FTIR (Fig. 3). As displayed, the characteristic bands at around 1785 cm^{-1}, 1706 cm^{-1} and 1367 cm^{-1} corresponded to the C═O asymmetric stretching, C═O symmetric stretching and C–N stretching in imide moieties, respectively, while the absorption peak at around 1660 cm^{-1} (C═O in amic acid) was hardly observed, confirming the successful synthesis of polyimide [31,32]. The bands at about 1303 cm^{-1} (imidazole breathing) and absence of the peaks corresponding to the imidazole NH stretching (3600-3000 cm^{-1}) further confirmed the successful incorporation of N-substituted imidazole ring [33,34]. Moreover, the polymer chain packing was estimated by WAXD (Fig. S4). In the result, all curves of the resulting PBII films exhibited a broad peak, exhibiting their amorphous character, which was different from the characteristics of the reported poly(benzimidazole imide)s with highly ordered molecular arrangements [28,29,35]. The fact indicated that the introduction of the askew and twisted segments was effective for loosening intermolecular packing.

3.3. Solubility

The solubility of poly(benzimidazole imide) films was evaluated in various organic solvents, as depicted in Table S2, which was found to drastically enhance in comparison with that of the previously reported PBIIs [22,27]. The cause was that the loose segment-chain packing, evidenced by the WAXD results, made it easy for solvent molecule to penetrate. Based on the analysis, the better solubility of 5b-based PBIIs compared to 5a-counterparts was contributed to the looser molecular packing came from the more noncoplanar conformation in the 5b-PBII series. On the other hand, 6FDA-PBIIs with lager structural distortions showed the similar trend in comparison with HPMDA-based ones in the result of Table S2 [36].

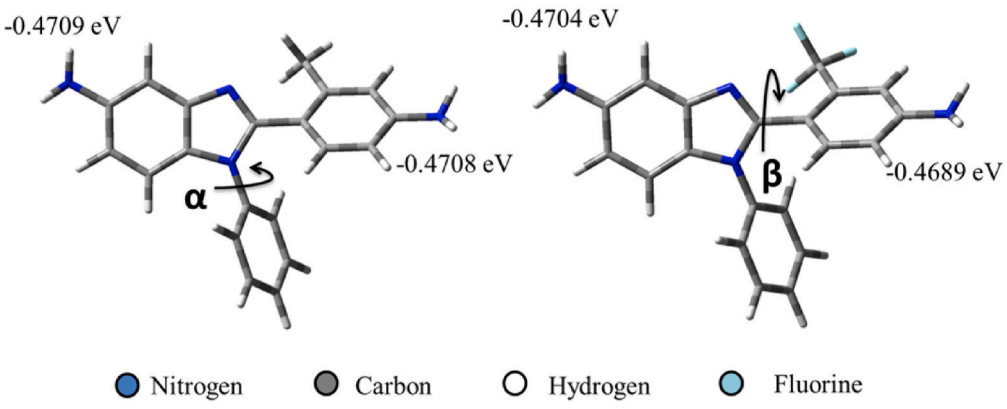

	α	β
5a	60°	44°
5b	60°	61°

Fig. 2. Optimized structures and net charges determined by the DFT [B3LYP/6-311G(d,p)].

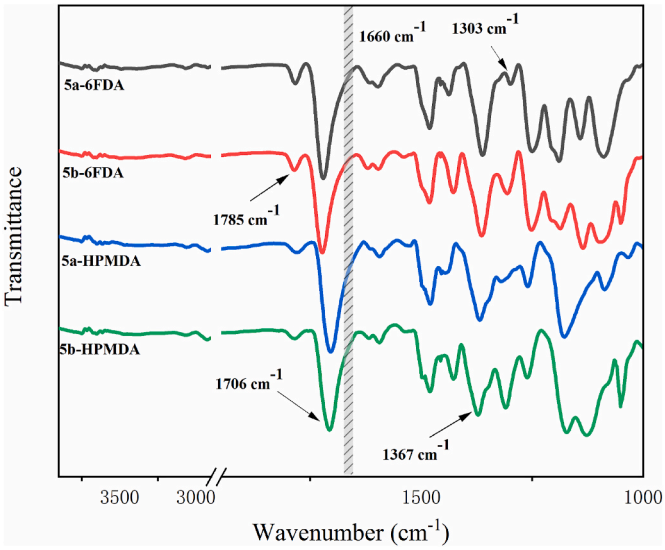

Fig. 3. ATR-FTIR spectra of the poly(benzimidazole imide) films.

3.4. Optical properties

The color intensity of polyimides was related to the intra- and inter-chain CT interactions which were susceptible to the structure of monomers and stacking of polymer backbone. Generally, the reduction of electron-donating ability (diamines), electron-accepting property (dianhydrides) and chain packing coefficient was helpful to inhibit CTC formation and further lightened the color of polyimide films [14,37]. In this work (Fig. 4 and Table 1), the cut-off wavelength ($\lambda_{cut\text{-}off}$) of these poly(benzimidazole imide)s was investigated to fall in the range 326–368 nm, which was superior to the reported PBII films [30]. The T_{400} values of the semi-aromatic PBIIs was higher than 80%, whereas the values for full-aromatic series was slightly inferior. The phenomenon was ascribed to the weak electron-withdrawing abilities of HPMDA, leading to reduced CT interactions. Moreover, the 5b-PBIIs demonstrated superior optical transparency compared to 5a-ones for certain dianhydrides. The observed phenomenon could be owing to that the presence of 2′-trifluoromethyl substituent in the N-phenyl benzimidazole diamine, which brought large amount of non-coplanar segments while reducing the monomer nucleophilicity, weakened the CTC formation. The trend was generally constant with the results of molecular modeling and ^{1}H NMR.

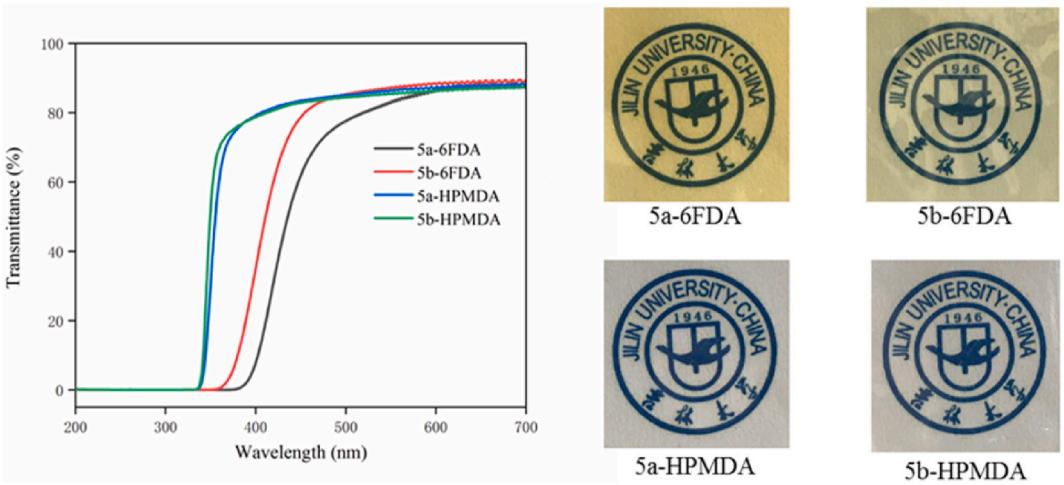

Fig. 4. UV–vis spectra and images of the poly(benzimidazole imide) films.

Table 1
Basic properties of the poly(benzimidazole imide) films.

Sample No.	T_g[a](°C)	$T_{d5\%}$[b](°C)	E(GPa)	σ(MPa)	ε(%)	CTE(ppm K^{-1})	$\lambda_{cut\text{-}off}$(nm)	T_{400}[c](%)
5a-6FDA	361	501	3.7	126	4.3	46	368	10
5b-6FDA	345	519	4.2	105	3.5	49	348	38
5a-HPMDA	402	454	3.1	113	7.0	42	342	80
5b-HPMDA	394	451	2.8	95	6.6	45	326	81

[a] Glass transition temperature measured by DMA at a heating rate of 5 °C min^{-1} at 1 Hz.
[b] 5% weight loss temperature measured by TGA in nitrogen at a heating rate of 10 °C min^{-1}.
[c] Transmittance at 400 nm.

The color intensities of the synthesized polyimides were investigated according to their lightness (L*), yellowness (b*), redness (a*) and yellowness index (YI). As shown in Table S3, the PBII films exhibited light colour with L* values of above 90, a* values of below 0, b* values from 1.94 to 26.49 and YI values in the range 3.84–16.79. The enhanced color intensities were attributed not only to the unsymmetrical structure but also to the highly twisted conformations coming from the synthesized diamine monomers. Among them, 4b-HPMDA displayed the lowest b* and YI values due to the nature of the 2′-CF_3 substituted diamine and alicyclic dianhydride which inhibited the formation of CTC.

3.5. Thermal properties

The TGA curves of the resulted PBIIs were displayed in Fig. 5, and the thermal analysis data was summarized in Table 1. Their 5% weight loss ranged from 451 to 519 °C confirmed the attractive thermal stability of these modified polyimides. Because greater chain conjugation and rigidity facilitated heat conduction, introduction of rigid backbone resulted in higher thermal decomposition temperature compared to those of the PIs containing flexible bonds [38,39]. Herein, the rodlike and rigid structures of these benzimidazole diamines enabled the corresponding PBIIs to inherit the heat-resistant advantages of highly rigid polyimide. And yet the thermal stability of the semi-aromatic PBIIs decreased to some degree with the use of HPMDA, which was related to the alicyclic unit that improved the possibilities of polymer backbone scission during high temperatures. However, their thermal stability ($T_{d5\%} \geq 450$ °C) was sufficient for further use.

The T_g values of these poly(benzimidazole imide)s determined by the peak temperature of the tan delta curve were 345–402 °C based on the DMA analysis (Fig. 6, Table 1). As shown in Fig. 7, their glass transition temperatures were higher than those of most previously reported

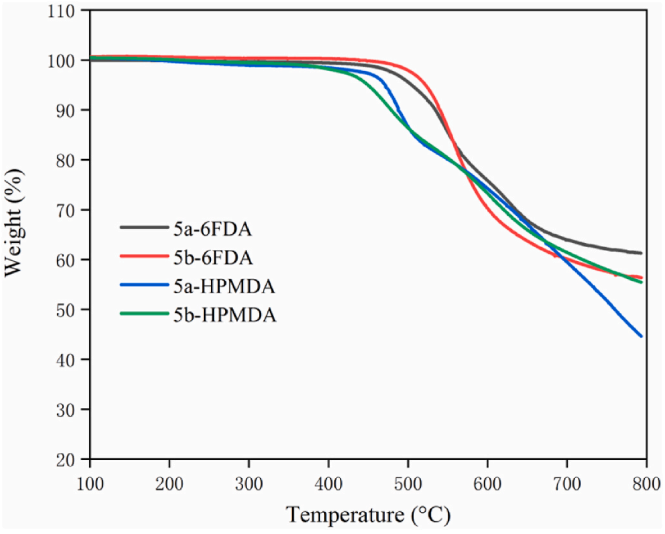

Fig. 5. TGA curves of the poly(benzimidazole imide) films under a nitrogen atmosphere.

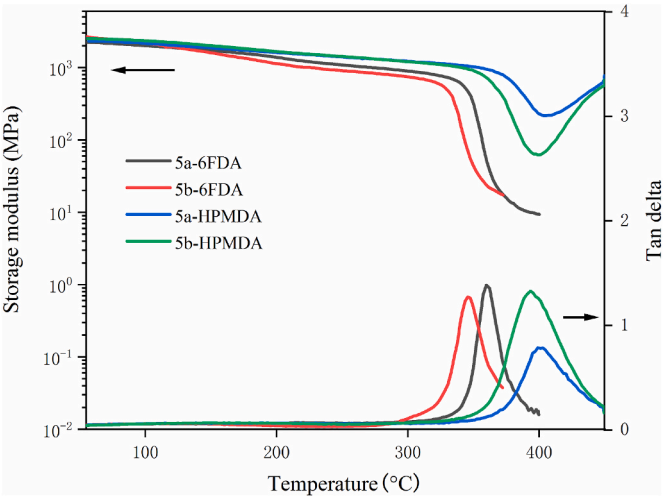

Fig. 6. DMA traces of the poly(benzimidazole imide) films.

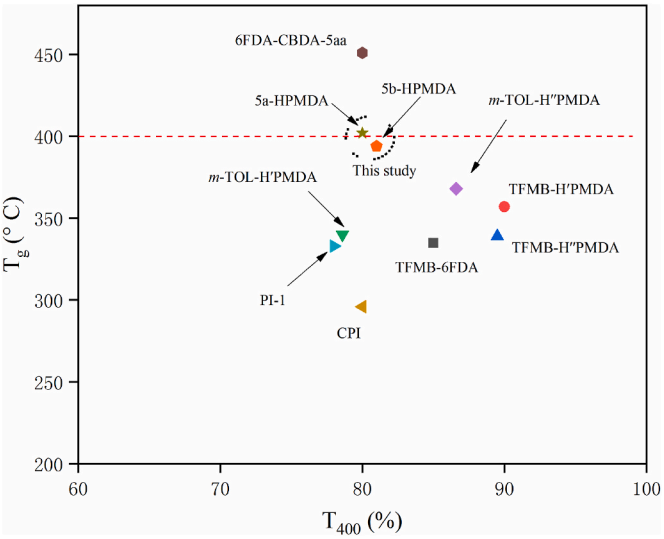

Fig. 7. Transparency-T_g diagram of reported colorless polyimides (TFMB-6FDA [40], TFMB-H′PMDA and *m*-TOL-H′PMDA [41], TFMB-H″PMDA and *m*-TOL-H″PMDA [42], CPI [43],PI-1 [44], 6FDA-CBDA-5aa [45]).

colorless polyimides [40–45]. This could be explained from two aspects. First, the askew diamine structure with significant steric hindrance tended to forbid the π-flip rotational motions of polymer chains when the temperature was close to the T_g [46]. Second, after the introduction of the rigid N-phenyl unit, its steric hindrance effectively limited the rotational freedom around polymer backbone [22,47]. Besides the geometrical factors of these diamines, the electron donation-acceptance interaction between segment-chains had a significant impact on T_g. In

general, such interaction was strengthened after the introduction of electron donating groups in the diamine moieties, and the corresponding T_g showed an upward trend. So the T_gs of 4a-PBIIs were 8–16 °C higher than those of 4b-based ones in the resulting system. Indeed, the HPMDA-derived polyimides displayed higher T_gs than the corresponding 6FDA-based ones. The phenomenon suggested that HPMDA was specifically effective for enhancing T_gs of polyimides, which was related to the "dish" shape of the alicyclic dianhydride that facilitating the close chain packing [37]. Thus, 5a-HPMDA displayed the highest T_g up to 402 °C.

The dimensional stability of these PBII films was measured by TMA. As depicted in Table 1, the CTE values arranged from 42 ppm K^{-1} to 49 ppm K^{-1}. Generally, higher degree of structural rigidity/linearity and stronger intermolecular interaction led to lower CTE [48,49]. In contrast to 5a, 5b possessed more twisted steric structures, further suppressing the polymer inter-molecular interactions. Thus, for the certain diamines, 5b-PBIIs had lower dimensional stability and higher CTE than 5a-PBIIs. Additionally, the presence of 6FDA was often responsible for a CTE increase, which originated from its nonlinear/non-coplanar structures. Herein, the polyimides from 6FDA exhibited relatively higher CTE values than the HPMDA-derived cases.

3.6. Mechanical properties

Fig. S5 and Table 1 summarized the mechanical properties of these PBII films. Essentially flexible PBIIs were formed with an initial modulus from 2.8 to 4.2 GPa, a tensile strength from 126 to 95 MPa, and an elongation at break in the ranges of 3.5–7.0%. In contrast, the full aromatic polyimides possessed higher tensile strength and modulus, whereas the semi-aromatic series displayed higher elongation at break. The superiority of the former was owing to their high molecular weights, but their rigid backbones resulted in brittle polymer films with insufficient chain entanglement, and that was, this type of PBIIs exhibited high mechanical properties with low toughness. The latter showed sufficient film flexibility as suggested from their very high ε_b values. On the other hand, the intermolecular interactions also played an important role in affecting mechanical properties, therefore, 5b-PBIIs with more distorted conformations had weaker chain-chain forces and tensile strengths in comparison with 5a-series. On the whole, their tensile strength (about 100 MPa) and initial modulus (exceed 2 GPa) was sufficient for the optical application [25].

4. Conclusions

Two new benzimidazole diamines and their polyimide films were synthesized. The analysis indicated that the introduction of twisted structures, which derived from the placement of appropriate substituents on the imidazole nitrogen and 2′-carbon atoms, reduced the chain-segments packing and intermolecular CT interaction to improve the optical properties of the PI films, for example, T_{400} = 80–81% and b* = 1.94–2.31 for 5a- and 5b-HPMDA. This series of chemical modifications did not change the rigid backbones of poly(benzimidazole imide) materials, which led to high thermal-resistance, including T_g up to 402 °C, and $T_{d5\%}$ over 450 °C. Among them, 5a-PBIIs displayed higher T_g than the corresponding 5b-ones because of the stronger inter-chain interaction, whereas the latter with their much non-planar fragments possessed higher transparency. In summary, the incorporation of N- and 2′-substituents can be used as an effective modification to improve the optical properties and maintain high thermostability of poly(benzimidazole imide)s, which provided new guides to design and prepare superheat-resistant colorless polymer films.

Declaration of competing interest

The authors declare that they have no known competing financial interests or personal relationships that could have appeared to influence the work reported in this paper.

Acknowledgement

This work was supported by the Key-Area Research and Development Program of Guangdong Province (2020B010182002).

Appendix A. Supplementary data

Supplementary data to this article can be found online at https://doi.org/10.1016/j.polymer.2022.125078.

References

[1] Y.W. Lim, J. Jin, B.S. Bae, Optically transparent multiscale composite films for flexible and wearable electronics, Adv. Mater. 32 (2020), 1907143.
[2] S. Haghanifar, A.J. Galante, P.W. Leu, Challenges and prospects of bio-inspired and multifunctional transparent substrates and barrier layers for optoelectronics, ACS Nano 14 (2020) 16241–16265.
[3] S. Nakano, N. Saito, K. Miura, T. Sakano, T. Ueda, K. Sugi, H. Yamaguchi, I. Amemiya, M. Hiramatsu, A. Ishida, Highly reliable a-IGZO TFTs on a plastic substrate for flexible AMOLED displays, J. Soc. Inf. Disp. 20 (2012) 493–498.
[4] M. Choi, Y. Kim, C. Ha, Polymers for flexible displays: from material selection to device applications, Prog. Polym. Sci. 33 (2008) 581–630.
[5] H. Ni, J. Liu, Z. Wang, S. Yang, A review on colorless and optically transparent polyimide films: chemistry, process and engineering applications, J. Ind. Eng. Chem. 28 (2015) 16–27.
[6] K.H. Nam, H.K. Choi, H. Yeo, N.H. You, B.C. Ku, J. Yu, Molecular design and property prediction of sterically confined polyimides for thermally stable and transparent materials, Polymers 10 (2018) 630.
[7] M.A. Abdulhamid, X. Ma, B.S. Ghanem, I. Pinnau, Synthesis and characterization of organo-soluble polyimides derived from alicyclic dianhydrides and a dihydroxyl functionalized spirobisindane diamine, ACS Appl. Polym. Mater. 1 (2019) 63–69.
[8] C.E. Sroog, Polyimides, Prog. Polym. Sci. 16 (1991) 561–694.
[9] M. Hasegawa, Y. Hoshino, N. Katsura, J. Ishii, Superheat-resistant polymers with low coefficients of thermal expansion, Polymer 111 (2017) 91–102.
[10] M. Ding, Isomeric polyimides, Prog. Polym. Sci. 32 (2007) 623–668.
[11] M. Hasegawa, K. Horie, Photophysics, photochemistry, and optical properties of polyimides, Prog. Polym. Sci. 26 (2001) 259–335.
[12] Y. Zhuang, J.G. Seong, Y.M. Lee, Polyimides containing aliphatic/alicyclic segments in the main chains, Prog. Polym. Sci. 92 (2019) 35–88.
[13] K. Kanosue, D. Peckus, R. Karpicz, T. Tamulevic, Polyimide and imide compound exhibiting bright red fluorescence with very large Stokes shifts via excited-state intramolecular proton transfer, Macromolecules 48 (2015) 1777–1785.
[14] S. Ando, T. Matsuura, S. Sasaki, Coloration of aromatic polyimides and electronic properties of their source materials, Polym. J. 29 (1997) 69–76.
[15] J. Miao, X. Hu, X. Wang, X. Meng, Z. Wang, J. Yan, Colorless polyimides derived from adamantane-containing diamines, Polym. Chem. 11 (2020) 6009–6016.
[16] M.A. Abdulhamid, G. Genduso, X. Ma, I. Pinnau, Synthesis and characterization of 6FDA/3,5-diamino-2,4,6-trimethylbenzenesulfonic acid-derived polyimide for gas separation applications, Separ. Purif. Technol. 257 (2021), 117910.
[17] M.A. Abdulhamid, G. Genduso, Y. Wang, X. Ma, I. Pinnau, Plasticization-resistant carboxyl-functionalized 6FDA-polyimide of intrinsic microporosity (PIM−PI) for membrane-based gas separation, Ind. Eng. Chem. Res. 59 (2020) 5247–5256.
[18] X. Hu, J. Yan, Y. Wang, H. Mu, Z. Wang, H. Cheng, F. Zhao, Z. Wang, Colorless polyimides derived from 2R,5R,7S,10S-naphthanetetracarboxylic dianhydride, Polym. Chem. 8 (2017) 6165–6172.
[19] Z. Mi, Z. Liu, J. Yao, C. Wang, C. Zhou, D. Wang, X. Zhao, H. Zhou, Y. Zhang, C. Chen, Transparent and soluble polyimide films from 1,4:3,6-dianhydro-D-mannitol based dianhydride and diamines containing aromatic and semiaromatic units: preparation, characterization, thermal and mechanical properties, Polym. Degrad. Stabil. 151 (2018) 80–89.
[20] L. Zhai, S. Yang, L. Fan, Preparation and characterization of highly transparent and colorless semi-aromatic polyimide films derived from alicyclic dianhydride and aromatic diamines, Polymer 53 (2012) 3529–3539.
[21] Y. Liu, Z. Zhou, L. Qu, B. Zou, Z. Chen, Y. Zhang, S. Liu, Z. Chi, X. Chen, J. Xu, Exceptionally thermostable and soluble aromatic polyimides with special characteristics: intrinsic ultralow dielectric constant, static random access memory behaviors, transparency and fluorescence, Mater. Chem. Front. 1 (2017) 326–337.
[22] H. Choi, I.S. Chung, K. Hong, C.E. Park, S.Y. Kim, Soluble polyimides from unsymmetrical diamine containing benzimidazole ring and trifluoromethyl pendent group, Polymer 49 (2008) 2644–2649.
[23] L. Luo, Y. Dai, Y. Yuan, X. Wang, X. Liu, Control of head/tail isomeric structure in polyimide and isomerism-derived difference in molecular packing and properties, macromol, Rapid Commun 38 (2017), 1700404.
[24] G. Qian, H. Chen, G. Song, F. Dai, J. Yao, Superheat-resistant polyimides with ultra-low coefficients of thermal expansion, Polymer 196 (2020), 122482.
[25] M. Lian, X. Lu, Q. Lu, Synthesis of superheat-resistant polyimides with high T_g and low coefficient of thermal expansion by introduction of strong intermolecular interaction, Macromolecules 51 (2018) 10127–10135.
[26] Y. Zhuang, X. Liu, Y. Gu, Molecular packing and properties of poly (benzoxazole-benzimidazole-imide) copolymers, Polym. Chem. 3 (2012) 1517–1525.

[27] M. Hasegawa, Y. Hoshino, N. Katsura, J. Ishii, Superheat-resistant polymers with low coefficients of thermal expansion, Polymer 111 (2017) 91–102.
[28] S. Wang, H. Zhou, G. Dang, C. Chen, Synthesis and characterization of thermally stable, high-modulus polyimides containing benzimidazole moieties, J. Polym. Sci., Part A: Polym. Chem. 47 (2009) 2024–2031.
[29] L. Luo, J. Yao, X. Wang, K. Li, J. Huang, B. Li, X. Liu, The evolution of macromolecular packing and sudden crystallization in rigid-rod polyimide via effect of multiple H-bonding on charge transfer (CT) interactions, Polymer 55 (2014) 4258–4269.
[30] G. Qian, F. Dai, H. Chen, M. Wang, M. Hu, C. Chen, Y. Yu, Incorporation of N-phenyl in poly(benzimidazole imide)s and improvement in H_2O-absorbtion and transparency, RSC Adv. 11 (2021) 3770–3776.
[31] Y.K. Xu, M.S. Zhan, K. Wang, Structure and properties of polyimide films during a far-infrared-induced imidization process, J. Polym. Sci., Part B: Polym. Phys. 42 (2004) 2490–2501.
[32] S. Diaham, M.L. Locatelli, T. Lebey, D. Malec, Thermal imidization optimization of polyimide thin films using Fourier transform infrared spectroscopy and electrical measurements, Thin Solid Films 519 (2011) 1851–1856.
[33] P. Musto, F.E. Karasz, W.J. MacKnight, Fourier transform infra-red spectroscopy on the thermo-oxidative degradation of polybenzimidazole and of a polybenzimidazole/polyetherimide blend, Polymer 34 (1993) 2934–2945.
[34] S. Qing, W. Huang, D. Yan, Synthesis and characterization of thermally stable sulfonated polybenzimidazoles obtained from 3,3′-disulfonyl-4,4′-dicarboxyldiphenylsulfone, J. Polym. Sci., Part A: Polym. Chem. 43 (2005) 4363–4372.
[35] G. Song, X. Zhang, D. Wang, X. Zhao, H. Zhou, C. Chen, G. Dang, Negative in-plane CTE of benzimidazole-based polyimide film and its thermal expansion behavior, Polymer 55 (2014) 3242–3246.
[36] Y. Zhuang, R. Orita, E. Fujiwara, Y. Zhang, S. Ando, Colorless partially alicyclic polyimides based on Tröger's base exhibiting good solubility and dual fluorescence/phosphorescence emission, Macromolecules 52 (2019) 3813–3824.
[37] F. Li, S. Fang, J.J. Ge, P.S. Honigfort, J.C. Chen, F.W. Harris, S.Z.D. Cheng, Diamine architecture effects on glass transitions, relaxation processes and other material properties in organo-soluble aromatic polyimide films, Polymer 40 (1999) 4571–4583.
[38] Y.N. Sazanov, F.S. Florinsky, M.M. Koton, Investigation of thermal and thermooxidative degradation of some polyimides containing oxyphenylene groups in the main chain, Eur. Polym. J. 15 (1979) 781–786.
[39] J. Lin, D.C. Sherrington, Recent developments in the synthesis, thermostability and liquid crystal properties of aromatic polyamides, Adv. Polym. Sci. 111 (1994) 177–219.
[40] T. Matsuura, Y. Hasuda, S. Nishi, N. Yamada, Polyimide derived from 2,2′-bis (trifluoromethyl)-4,4′-diaminobiphenyl. 1. Synthesis andcharacterization of polyimides prepared with 2,2′-bis(3,4-dicarboxyphenyl)hexafluoropropane dianhydride orpyromellitic dianhydride, Macromolecules 24 (1991) 5001–5005.
[41] M. Hasegawa, M. Fujii, J. Ishii, S. Yamaguchi, E. Takezawa, T. Kagayama, A. Ishikawa, Colorless polyimides derived from 1S,2S,4R,5R-cyclohexanetetracarboxylic dianhydride, self-orientation behavior during solution casting, and their optoelectronic applications, Polymer 55 (2014) 4693–4708.
[42] M. Hasegawa, D. Hirano, M. Fujii, M. Haga, E. Takezawa, S. Yamaguchi, A. Ishikawa, T. Kagayama, Solution-processable colorless polyimides derived from hydrogenated pyromellitic dianhydride with controlled steric structure, J. Polym. Sci., Part A: Polym. Chem. 51 (3) (2013) 575–592.
[43] H. Zuo, G. Qian, H.B. Li, F. Gan, Y. Fang, X. Li, J. Dong, X. Zhao, Q. Zhang, Reduced coefficient of linear thermal expansion for colorless and transparent polyimide by introducing rigid-rod amide units: synthesis and properties, Polym. Chem. 13 (2022) 2999–3008.
[44] H. Zuo, Y. Chen, G. Qian, F. Yao, H. Li, J. Dong, X. Zhao, Q. Zhang, Effect of simultaneously introduced bulky pendent group and amide unit on optical transparency and dimensional stability of polyimide film, Eur. Polym. J. 173 (2022), 111317.
[45] P. Xiao, X. He, F. Zheng, Q. Lu, Super-heat resistant, transparent and low dielectric polyimides based on spirocyclic bisbenzoxazole diamines with $T_g > 450$ °C, Polym. Chem. (2022), https://doi.org/10.1039/D2PY00513A.
[46] T. Okada, R. Ishige, S. Ando, Effects of chain packing and structural isomerism on the anisotropic linear and volumetric thermal expansion behaviors of polyimide films, Polymer 146 (2018) 386–395.
[47] Z. Sun, M. Liu, L. Yi, Y. Wang, High glass transition of organo-soluble copolyimides derived from a rigid diamine with tert-butyl-substituted triphenylpyridine moiety, RSC Adv. 3 (2013) 7271–7276.
[48] J.H. Jou, P.T. Huang, Effect of thermal curing on the structures and properties of aromatic polyimide films, Macromolecules 24 (1991) 3796–3803.
[49] M. Hasegawa, K. Okuda, M. Horimoto, Y. Shindo, R. Yokota, M. Kochi, Spontaneous molecular orientation of polyimides induced by thermal imidization. 3. Component chain orientation in binary polyimide blends, Macromolecules 30 (1997) 5745–5752.